J. Eukaryot. Microbiol., 53(4), 2006 pp. 280–291

DOI: 10.1111/j.1550-7408.2006.00109.x

Cellular Identity of a Novel Small Subunit rDNA Sequence Clade of Apicomplexans: Description of the Marine Parasite *Rhytidocystis polygordiae* n. sp. (Host: *Polygordius* sp., Polychaeta)

BRIAN S. LEANDER[a] **and PATRICIA A. RAMEY**[b]

[a]*Canadian Institute for Advanced Research, Program in Evolutionary Biology, Departments of Botany and Zoology, University of British Columbia, Vancouver, BC, Canada V6T 1Z4, and*
[b]*Institute of Marine and Coastal Sciences, Rutgers University, New Jersey 08901, USA*

ABSTRACT. A new species of *Rhytidocystis* (Apicomplexa) is characterized from North American waters of the Atlantic Ocean using electron microscopy and phylogenetic analyses of small subunit (SSU) rDNA sequences. *Rhytidocystis polygordiae* n. sp. is a parasite of the polychaete *Polygordius* sp. and becomes the fourth described species within this genus. The trophozoites of *R. polygordiae* were relatively small oblong cells ($L = 35–55$ μm; $W = 20–25$ μm) and distinctive in possessing subterminal indentations at both ends of the cell. The surface of the trophozoites had six to eight longitudinal series of small transverse folds and several micropores arranged in short linear rows. The trophozoites of *R. polygordiae* were positioned beneath the brush border of the intestinal epithelium but appeared to reside between the epithelial cells within the extracellular matrix rather than within the cells. The trophozoites possessed a uniform distribution of paraglycogen granules, putative apicoplasts, mitochondria with tubular cristae, and a centrally positioned nucleus. The trophozoites were non-motile and lacked a mucron and an apical complex. Intracellular sporozoites of *R. polygordiae* had a conoid, a few rhoptries, micronemes, dense granules, and a posteriorly positioned nucleus. Phylogenies inferred from SSU rDNA sequences demonstrated a close relationship between *R. polygordiae* and the poorly known parasite reported from the hemolymph of the giant clam *Tridacna crocea*. The rhytidocystid clade diverged early in the apicomplexan radiation and showed a weak affinity to a clade consisting of cryptosporidian parasites, monocystids, and neogregarines.

Key Words. Agamococcidia, Apicomplexa, apicoplast, archiannelids, Coccidia *Cryptosporidium*, gregarines, molecular phylogeny, *Rhytidocystis*, ultrastructure.

APICOMPLEXAN diversity is just beginning to be explored with molecular phylogenetic approaches, especially for groups that do not have a direct impact on human welfare. Most likely, tens of thousands of apicomplexan species remain undiscovered, especially those that inhabit marine environments. An improved understanding of these lineages should shed considerably more light on the unity and diversity of apicomplexan parasites and the earliest stages in the evolution of parasitism in the group (Leander and Keeling 2004; Leander et al. 2006). Perhaps the least understood members of the Apicomplexa are gregarines and several enigmatic coccidian-like lineages with uncertain phylogenetic position. The ''Agamococcidiorida'' is an enigmatic and ill-named group of apicomplexans first recognized by Levine (1979) because these organisms have eucoccidian-like cyst characteristics (e.g. oocysts containing sporocysts, each containing two sporozoites) but seem to lack gamonts, merogony, and any evidence of sexual reproduction. Most ''agamococcidians'' have relatively large trophozoites, a general feature of many marine gregarines. Unlike most gregarines, however, the trophozoites of ''agamococcidians'' are non-motile and reside within the extracellular spaces of host epithelial tissues. This unique combination of features is significant from an evolutionary perspective because a better understanding of these parasites could provide important insights into the deep relationships among gregarines, cryptosporidian parasites, and eucoccidians.

Rhytidocystis and *Gemmocystis* are the only described ''agamococcidian'' genera (Levine 1979; Upton and Peters 1986). The latter contains a single species, *Gemmocystis cylindrus*, described from the gastrodermis of scleractinian corals (Upton and Peters 1986). *Rhytidocystis* comprises three species, all of which were collected from polychaetes in European waters of the eastern Atlantic Ocean (de Beauchamp 1913; Porchet-Hennere 1972). Here we describe a new rhytidocystid species that parasitizes *Polygordius*, a meiofaunal polychaete from North American waters of the western Atlantic Ocean (Ramey, Fiege, and Leander 2006). Our ultrastructural and molecular phylogenetic data help clarify the cellular identity of *Rhytidocystis*, and a poorly understood parasite of the giant clam *Tridacna crocea*. Moreover, these data uncover another clade of enigmatic parasites that diverges early in the apicomplexan radiation.

Corresponding Author: B. Leander, Canadian Institute for Advanced Research, Program in Evolutionary Biology, Departments of Botany and Zoology, University of British Columbia, Vancouver, BC V6T 1Z4 Canada—Telephone number: 604-822-2474; FAX number: 604-822-6089; e-mail: bleander@interchange.ubc.ca

MATERIALS AND METHODS

Collection of organisms. Trophozoites of *Rhytidocystis polygordiae* n. sp. were isolated from the intestinal epithelium of the polychaete *Polygordius* sp. Ramey, 2006. Host worms were collected during the spring and summer months of 2004/05 by SCUBA divers near Station 9 at the LEO-15 research site on Beach Haven Ridge, NJ (39°28′ N, 74°15′ W) (Ramey et al. 2006; Von Alt and Grassle 1992).

Microscopy. Host dissections and micromanipulation of individual parasites were conducted with a Leica MZ6 stereomicroscope and a Zeiss Axiovert 200 inverted microscope. Differential interference contrast (DIC) light micrographs were produced by securing parasites under a cover slip with vaseline and viewing them with a Zeiss Axioplan 2 imaging microscope connected to a Leica DC500 color digital camera.

Parasites were released into seawater by teasing apart the host with fine-tipped forceps. Fifteen individual parasites were removed from the macerated tissue by micromanipulation and washed twice in filtered seawater. As described previously (Leander, Harper, and Keeling 2003b), washed parasites were deposited directly into the threaded hole of a Swinnex filter holder, containing a 5-μm polycarbonate membrane filter (Coring Separations Division, Acton, MA) submerged in seawater within a small canister. Whatman filter paper, mounted on the inside of a beaker, was used to fix the parasites with OsO_4 vapors for 30 min. Five drops of 4% (w/v) OsO_4 were added directly to the seawater and the trophozoites were fixed for an additional 30 min. The trophozoites were dehydrated with a graded series of ethyl alcohol

and critical point dried with CO_2. Filters were mounted on stubs, sputter coated with gold, and viewed under a Hitachi S4700 Scanning Electron Microscope. Some SEM images were illustrated on a black background using Adobe Photoshop 6.0 (Adobe Systems, San Jose, CA).

Transmission electron microscopy (TEM) was conducted on parasites in situ. Fragments of host worms were collected in Eppendorf tubes and fixed in a 2% (v/v) glutaraldehyde in seawater at 4 °C for 1 h. The fixed worms were washed twice in seawater for 15 min and post-fixed with 1% (w/v) OsO_4/seawater cocktail at 4 °C for 1 h. Worm fragments were dehydrated with a graded series of ethyl alcohol and acetone, infiltrated with acetone-resin mixtures, and flat embedded with pure Epon resin at 60 °C. Worm fragments were excised with a razor blade and glued to Epon blocks. Ultrathin sections were generated using a Leica Ultracut T Ultramicrotome, post-stained with uranyl acetate and lead citrate, and viewed under a Hitachi H7600 Transmission Electron Microscope.

DNA isolation, PCR, cloning, and sequencing. Thirty-five trophozoites were manually isolated from dissected hosts, washed three times in filtered seawater, and deposited into 1.5 ml Eppendorf tubes. DNA was extracted with a standard CTAB extraction protocol: pelleted parasites were suspended in 200 µl CTAB extraction buffer (1.12 g Tris, 8.18 g NaCl, 0.74 g EDTA, 2 g CTAB, 2 g polyvinylpyrolidone, 0.2 ml 2-mercaptoethanol in 100 ml water) and incubated at 65 °C for 30 min. DNA was separated with chloroform:isoamyl alcohol (24:1). The aqueous phase was then precipitated in 70% ethanol.

The small subunit (SSU) rRNA gene from *R. polygordiae* n. sp. was amplified as a single fragment using universal eukaryotic PCR primers 5′-CGAATTCAACCTGGTTGATCCTGCCAGT-3′ and 5′-CCGGATCCTGATCCTTCTGCAGGTTCACCTAC-3′ (Leander, Clopton, and Keeling 2003a). PCR products corresponding to the expected size were gel isolated and cloned into the pCR 2.1 vector using the TOPO TA cloning kit (Invitrogen, Frederick, MD). Eight cloned plasmids were digested with *EcoR1* and screened for size. Two clones were sequenced with ABI bigdye reaction mix using vector primers oriented in both directions. The SSU rDNA sequence was identified by BLAST analysis and deposited in GenBank (Accession number DQ273988).

Molecular phylogenetic analysis. The new sequence from *R. polygordiae* n. sp. was aligned with 55 other alveolate SSU rDNA sequences using MacClade 4 (Maddison and Maddison 2000) and visual fine-tuning. The sequences from *Selenidium vivax* (AY196708) and the apicomplexan sequence misattributed to the foraminiferan *Ammonia beccarii* (U07937) were omitted from the analyses in order to circumvent long-branch attraction (LBA) artifacts and because the latter sequence is missing data (Leander et al. 2003a, b; Wray et al. 1995). Maximum likelihood (ML) and distance methods under different DNA substitution models were performed on the 56-taxon alignment containing 1,159 unambiguously aligned sites; all gaps were excluded from the alignment before phylogenetic analysis. The α shape parameters were estimated from the data using HKY and a gamma distribution with invariable sites and eight rate categories ($\alpha = 0.38$; Ti/Tv = 1.85; fraction of invariable sites = 0.02). Gamma-corrected ML trees (analyzed using the α shape parameter listed above) were constructed with PAUP* 4.0 using the general time reversible (GTR) model for base substitutions (Posada and Crandall 1998; Swofford 1999). Gamma-corrected ML tree topologies found with HKY and GTR were identical. ML bootstrap analyses were performed in PAUP* 4.0 (Swofford 1999) on 100 re-sampled datasets under a HKY model using the α shape parameter and transition/transversion (Ti/Tv) ratio estimated from the original dataset.

Distances for the SSU rDNA dataset were calculated with TREE-PUZZLE 5.0 using the HKY substitution matrix (Strimmer and Von Haeseler 1996) and trees were constructed with weighted neighbor joining (WNJ) using Weighbor (Bruno, Socci, and Halpern 2000). Five-hundred bootstrap datasets were generated with SEQBOOT (Felsenstein 1993). Respective distances were calculated with the shell script ''puzzleboot'' (M. Holder and A. Roger, www.tree-puzzle.de) using the α shape parameter and Ti/Tv ratios estimated from the original dataset and analyzed with Weighbor.

We also examined the 56-taxon dataset with Bayesian analysis using the program MrBayes 3.0 set to operate with GTR, a γ distribution, and four MCMC chains (default temperature = 0.2) (Huelsenbeck and Ronquist 2001). A total of 2,000,000 generations were calculated with trees sampled every 100 generations and with a prior burn-in of 200,000 generations (2,000 sampled trees were discarded). A majority rule consensus tree was constructed from 16,000 post-burn-in trees with PAUP* 4.0. Posterior probabilities correspond to the frequency at which a given node is found in the post-burn-in trees.

GenBank accession numbers. *Adelina bambarooniae* (AF494059), *Amphidinium asymmetricum* (AF274250), *Babesia bigemina* (AY603402), *Rhytidocystis polygordiae* (DQ273988), *Blepharisma americanum* (M97909), *Colpoda inflata* (M97908), *Colpodella edax* (AY234843), *Colpodella pontica* (AY078092), *Colpodella tetrahymenae* (AF330214), *Cryptosporidium baileyi* (L19068), *Crypthecodinium cohnii* (M64245), *Cryptosporidium parvum* (AF093489), *Cryptosporidium serpentis* (AF093502), *Cytauxzoon felis* (AF39993), *Eimeria tenella* (U67121), Environmental sequences (AF372772, AF372779, AF372780, AF372785, AF372786, AY179975, AY179976, AY179977, AY179988), *Gonyaulax spinifera* (AF022155), *Gregarina niphandrodes* (AF129882), *Gymnodinium sanguineum* (AJ415513), *Gyrodinium dorsum* (AF274261), *Hematodinium* sp. (AF286023), *Hepatozoon catesbianae* (AF130361), *Kryptoperidinium foliaceum* (AF274268), *Lankesteria abbotti* (DQ093796), *Lankesterella minima* (AF080611), *Lecudina polymorpha* morphotype 1 (AY196706), *Lecudina tuzetae* (AF457128), *Leidyana migrator* (AF457130), *Lessardia elongata* (AF521100), *Lithocystis* sp. (DQ093795), Marine parasite from *T. crocea* (AB000912), *Mattesia geminata* (AY334568), *Monocystis agilis* (AF457127), *Neospora caninum* (AJ271354), *Noctiluca scintillans* (AF022200), *Ophryocystis elektroscirrha* (AF129883), *Oxytricha nova* (M14601), *Paramecium tetraurelia* (X03772), *Perkinsus marinus* (AF126013), *Pfiesteria piscicida* (AY033488), *Prorocentrum panamensis* (Y16233), *Pterospora floridiensis* (DQ093794), *Pterospora schizosoma* (DQ093793), *Sarcocystis muris* (M64244), *Scrippsiella sweeneyae* (AF274276), *Selenidium terebellae* (AY196709), *Theileria parva* (AF013418), *Toxoplasma gondii* (M97703).

Taxon Description

Apicomplexa Levine 1970
***Rhytidocystis polygordiae* Leander et Ramey n. sp.**

Diagnosis. Relatively small oblong trophozoites about 50 µm in length and 20 µm in width. Trophozoites without mucron or apical complex and symmetrical along the mid-sagittal and mid-transverse planes. Trophozoites with centrally positioned nucleus and subterminal indentations at both, otherwise rounded, ends of the cell. Trophozoite surface often with six to eight longitudinal series of small transverse folds and short linear rows of six or more micropores. Trophozoites with four membrane-bound organelles (putative apicoplasts), as well as a uniform accumulation of paraglycogen granules and lipid droplets within the cytoplasm. Trophozoites without cell motility, positioned beneath the brush border, and apparently within the extracellular matrix of the host's

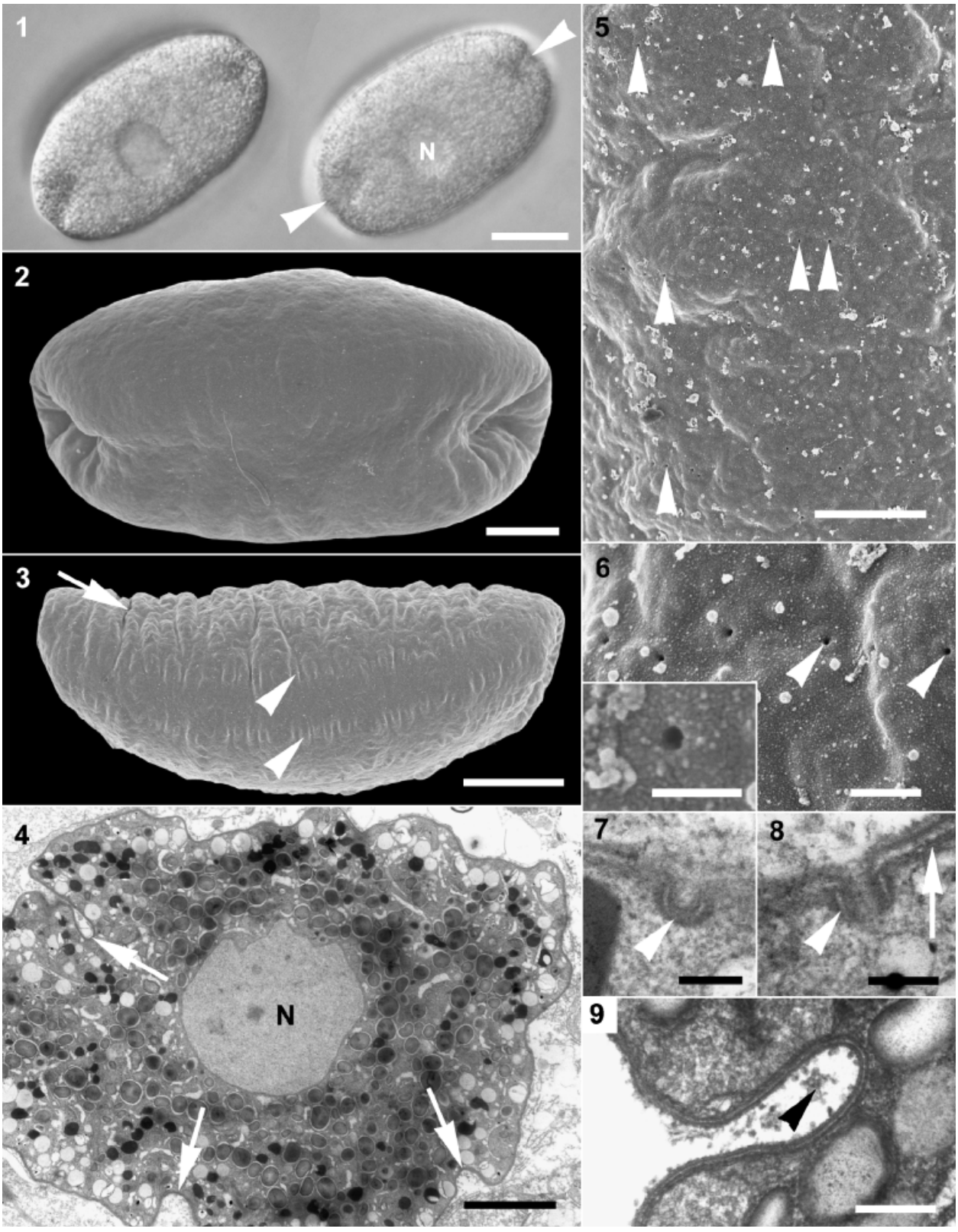
1
N
2
3
4
N
5
6
7
8
9

Table **1.** Comparison of morphological character states in rhytidocystids, including *Rhytidocystis polygordiae* n. sp. (de Beauchamp 1913; Levine 1979; Porchet-Hennere 1972).

Characters	*R. polygordiae*	*R. opheliae*	*R. henneguyi*	*R. sthenelais*
Host (Polychaeta)	*Polygordius* sp.	*Ophelia bicornis*	*Ophelia neglecta*	*Sthenelais boa*
Habitat	W. Atlantic	E. Atlantic	E. Atlantic	E. Atlantic
Trophozoites				
Shape	Oblong	Flat oval	Flat oval	Unknown
Size ($L \times W$, μm)	50 × 20	400 × 300	310 × 220	Unknown
Motility	None	None	None	Unknown
Transverse surface folds	Yes	Yes	Unknown	Unknown
Nucleus				
Heterochromatin	No	Unknown	Unknown	Unknown
Location	Central	Central	Central	Unknown
Apical complex/mucron	No	No	No	Unknown
Putative apicoplasts	Yes	Unknown	Unknown	Unknown
Terminal concavities	Yes	No	No	Unknown
Host issue	Intestine	Coelom	Intestine/coelom	Unknown
Position in host	Subepithelial	Subepithelial	Subepithelial	Unknown
Gamonts	None	None	None	Unknown
Oocysts	Yes—coelom	Yes—coelom	Yes—coelom	Yes—coelom
Sporozoites				
No. per sporocyst	Unknown	2	2	2
Shape	Spindle	Spindle	Spindle	Spindle
Size ($L \times W$, μm)	12 × 2	10 × 2	10 × 2	10 × 2
Nucleus				
Heterochromatin	Yes	Unknown	Unknown	Yes
Location	Posterior	Posterior	Posterior	Posterior
Conoid & rhoptries	Yes	Yes	Yes	Yes
Putative apicoplasts	Unknown	Unknown	Unknown	Yes
Crystalloid bodies	No	Unknown	Unknown	Yes

intestinal epithelium. Cysts within coelom. Intracellular sporozoites spindle-shaped and about 12 μm long and 2 μm wide. Sporozoites with posterior nucleus, conoid, polar ring, rhoptries, and micronemes, but without micropores. Mitochondria of both sporozoites and trophozoites with tubular cristae.

Hapantotype. Both resin-embedded trophozoites used for TEM and trophozoites on gold sputter-coated SEM stubs have been deposited in the Beaty Biodiversity Research Centre (Marine Invertebrate Collection) at the University of British Columbia, Vancouver, Canada. The embedded trophozoites were fixed in situ within the host intestines.

Iconotype. Fig. 1–6 and 20–25.

Type locality. Western coast of the Atlantic Ocean near Beach Haven Ridge, NJ, USA (39°28′ N, 74°15′ W).

Habitat. Marine.

Etymology for the specific epithet. Refers to the genus of the host.

Type host. *Polygordius* sp. (Annelida, Polychaeta, Palpata, Canalipalpata, Polygordiidae).

Location in host. Intestinal epithelium.

RESULTS AND DISCUSSION

Comparative biology and ultrastructure. Our observations of the *Polygordius* parasites were most consistent with previous descriptions of species in the genus *Rhytidocystis* (see de Beauchamp 1913; Levine 1979; Porchet-Hennere 1972). The significant similarities and differences between *R. polygordiae* n. sp. and other closely related species are outlined in Table 1. A close relationship might also exist between the polychaete hosts of rhytidocystid parasites, reflecting the so-called ''Fahrenholz' rule'' (Hennig 1966). Of the three previously described rhytidocystid species, two of the hosts belong to the polychaete family Opheliidae, which has been suggested in several reports to be the sister group to Polygordiidae (Giard 1880; McIntosh 1875; Rouse and Pleijel 2001). We were able to characterize the trophozoites and putative sporozoites of *R. polygordiae*. The trophozoites of *R. polygordiae* were relatively small oblong cells ($L = 35–55$ μm; $W = 20–25$ μm; $n = 32$) with a central nucleus and shallow indentations at both, otherwise rounded, ends (Fig. 1, 2). Both ends of the cell were indistinguishable; there was no evidence of a mucron or apical complex. The indentations were positioned sub-terminally, and the

Fig. **1–9.** Light and electron micrographs of the trophozoite surface in *Rhytidocystis polygordiae* n. sp. **1.** Light micrographs showing the oblong cell shape, granular cytoplasm, central nucleus (N), and subterminal indentations (arrowheads) (Bar = 15 μm). **2.** Scanning electron micrograph (SEM) of a trophozoite showing the subterminal indentations oriented downwards, which defines the ventral surface of trophozoites (Bar = 5 μm). **3.** SEM showing a trophozoite in lateral view (ventral surface oriented downwards) and longitudinal rows of small transverse folds (arrowheads). Deeper oblique folds were evident on the dorsal surface (arrow) (Bar = 10 μm). **4.** Transmission electron micrograph (TEM) through a trophozoite showing deep oblique folds (arrows) and a large central nucleus (N) lacking condensed heterochromatin (Bar = 4 μm). **5.** SEM showing a scattered distribution of pellicular pores (Bar = 2.5 μm). **6.** Higher magnification SEM showing a linear arrangement of pellicular pores oriented transversely over the trophozoite surface (Bar = 0.5 μm). **Inset:** High magnification SEM of a pellicular pore (Bar = 0.2 μm). **7.** Oblique TEM through a pellicular pore (arrowhead) (Bar = 0.2 μm). **8.** Transverse TEM trough a pellicular pore (arrowhead) showing that the pores are defined by and continuous with the inner membrane complex (arrow) (Bar = 0.2 μm). **9.** Higher magnification TEM of a deep oblique fold showing extracellular material (arrowhead) and the typical tripartite construction of the apicomplexan pellicle: plasma membrane + the two membranes of the inner membrane complex (Bar = 0.5 μm).

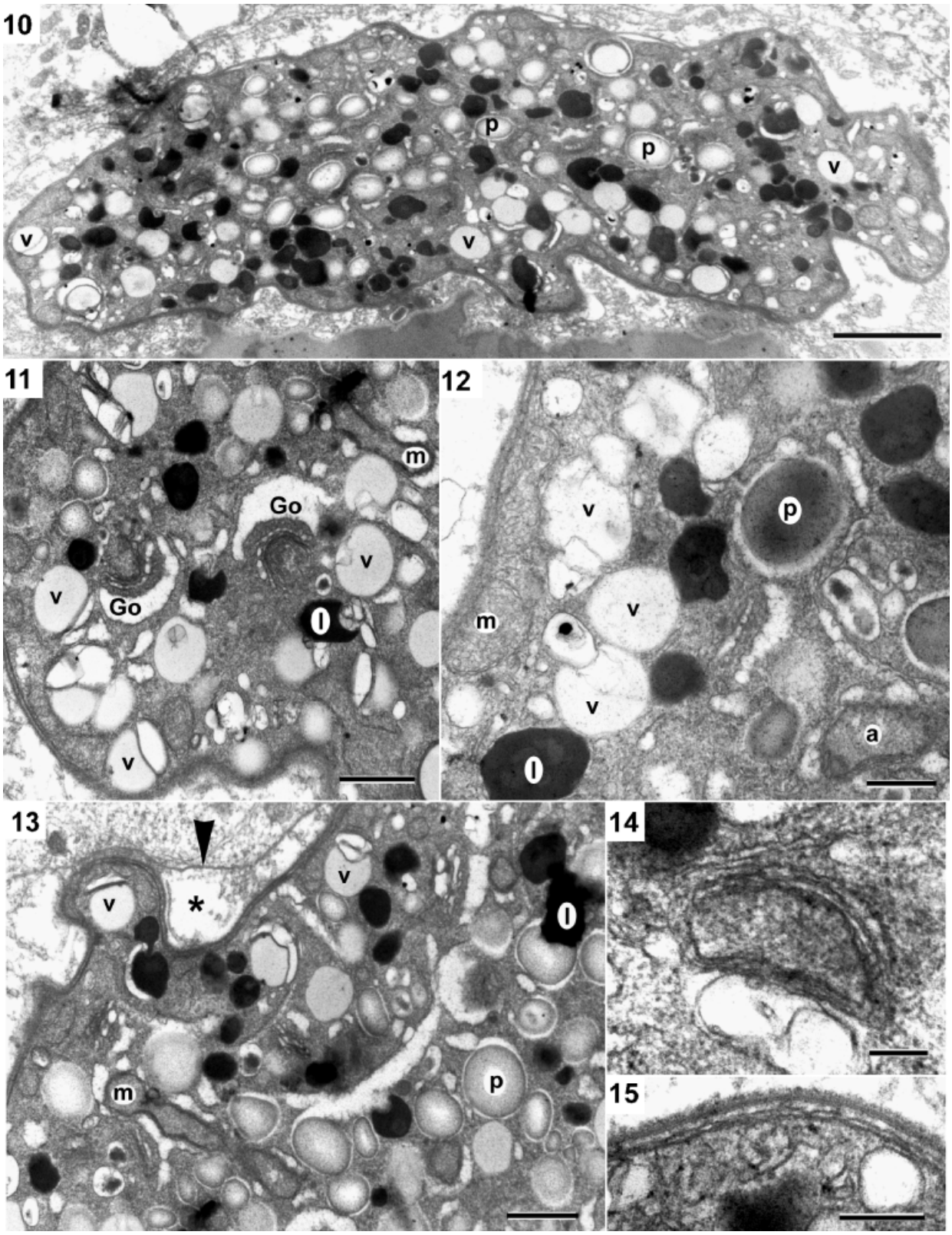
10
p
p
v
v
v
11
m
Go
v
v
Go
l
v
12
v
p
m
v
v
a
l
13
v
*
v
l
m
p
14
15

''downward'' orientation of both indentations permitted us to define the ventral surface of the trophozoites (Fig. 2). Some trophozoites (four of 10 cells observed with the SEM) possessed longitudinal rows of small transverse folds, a surface pattern that was reminiscent of *Rhytidocystis opheliae* (de Beauchamp 1913; Levine 1979; Porchet-Hennere 1972). The number of these longitudinal rows ranged from six to eight in *R. polygordiae*, which stands in contrast to the approximately 30 longitudinal rows reported in *R. opheliae*. Most of the trophozoites also possessed deeper oblique, or transverse, in-folds that appeared to be most common on the dorsal surface (Fig. 3, 4). The trophozoite surface was pierced by numerous micropores (diam. = 0.05–0.1 μm), which were often aligned in short linear rows of six or more pores (Fig. 5, 6). TEM demonstrated that the pores were continuous with the inner membrane complex (Fig. 7, 8). Because there is no apical complex present in the trophozoites for myzocytosis-based feeding (Leander and Keeling 2003; Schrével 1968), we infer that the pores function in nutrient uptake via endocytosis.

The nucleus and cytoplasm of the trophozoites were typical of most apicomplexans in appearance and organization. The cell surface had the usual apicomplexan organization of a plasma membrane subtended by an inner membrane complex of two closely packed membranes (Fig. 15). The large central nuclei were homogeneous in appearance and generally lacked condensed heterochromatin (Fig. 4). The cytoplasm of the trophozoites was filled with five major elements: reserve granules, mitochondria, lipid droplets, vacuoles, and Golgi bodies. The reserve granules were similar in shape (semi-spherical), size (diam. = 0.5–1.0 μm), distribution, and appearance to the paraglycogen granules observed in many gregarines (Fig. 4, 10–13) (Landers 2002; Schrével 1971a, b; Vivier 1968; Vivier and Schrével 1966; Warner 1968). Mitochondrial profiles were common near the cell periphery and took on various shapes, ranging from spherical to irregularly elongate (Fig. 11–13). Like most members of the Alveolata, the mitochondria in *R. polygordiae* had tubular cristae. Darkly stained lipid droplets were distributed evenly throughout the cytoplasm (Fig. 4, 10). The Golgi bodies consisted of a crescent-shaped stack of two to four cisternae and were distinctive in having a large crescent-shaped vacuole near the trans-face (Fig. 11). Although similar structures were reported in the polychaete parasite *Coelotropha durchoni* (Vivier and Hennere 1965), it is unclear whether or not the Golgi-associated vacuoles in *R. polygordiae* are an artifact of fixation.

Although ultrastructural preservation was modest, there is compelling evidence that the trophozoites of *R. polygordiae* possess small organelles (diam. = 0.75 μm) bounded by four membranes (Fig. 12, 14). These organelles are similar in size and structure to the known vestigial plastids present in other apicomplexans, the so-called ''apicoplasts'' (Waller and McFadden 2005) (Fig. 12, 14). Apicoplasts appear to be widespread among apicomplexans, as these organelles have been found in several different groups of apicomplexans (Lang-Unnasch et al. 1998; McFadden et al. 1997; Oborník et al. 2002). One key exception is *Cryptosporidium parvum*, which appears to lack the organelle entirely (McFadden 2003; Zhu, Marchewka, and Keithly 2000). Apicoplasts have not been definitively shown in gregarines or gregarine-like apicomplexans, although a few ultrastructural studies have described ''mysterious'' four membrane-bound organelles in *Rhytidocystis sthenelais* (''agamococcidian''), *Coelotropha durchoni* (''protococcidian''), and *Selenidium pendula* (''archigregarine''), which are highly suggestive of apicoplasts (Porchet-Hennere 1972; Schrével 1971b; Vivier and Hennere 1965). Therefore, the presence of putative apicoplasts in *R. polygordiae* is not unexpected, but it does represent only the 4th report of four membrane-bound organelles in marine apicomplexans.

A fundamental characteristic used to discriminate between different groups of apicomplexans is the position of the parasites relative to the tissues of the host (e.g. extracellular versus intracellular) (Vivier and Desportes 1990). Most eugregarines possess large (>60 μm) motile trophozoites that occupy the extracellular body cavities of their hosts (e.g. intestinal lumen, coeloms, and reproductive vesicles). The dominant life stages of cryptosporidian parasites occupy an intracellular, but extracytoplasmic, position within the host intestinal epithelial cells (Chen et al. 2002; Elliot and Clark 2000; Petry 2004). Cryptosporidian parasites infect the distal edge of epithelial cells and form a quasi-extracellular bulge within the brush border. By contrast, the dominant life stages of most eucoccidians and piroplasmids are more noticeably intracellular, either within a parasitophorous vacuole, as in the former, or in direct contact with the cytoplasm of the host cell, as in the latter (Beyer et al. 2002). The trophozoites of *R. polygordiae* could be observed through the body wall of the host with light microscopy (Fig. 16). The parasites were usually arranged in clusters and pressed closely against the lining of the intestinal lumen. This locality is similar to *R. henneguyi* and might stand in contrast to *R. opheliae* and *R. sthenelais*, which apparently inhabit the peritoneal tissues around the coelom of their hosts (de Beauchamp 1913; Levine 1979) (Table 1). Like other *Rhytidocystis* species, neither gliding motility nor writhing motility was observed in trophozoites in situ or in trophozoites that were released from the intestines by micro-dissection. Low magnification TEMs showed that the trophozoites were not surrounded by a conspicuous parasitophorous vacuole, but they were positioned just beneath the brush border of the intestinal epithelium, giving the appearance of an intracellular localization (Fig. 17). Although inconclusive, higher magnification TEMs suggested that the trophozoites of *R. polygordiae* did not actually occupy an intracellular position, and instead were situated within the interstitial spaces between adjacent epithelial cells (Fig. 18, 19). In this context, the spaces created by the in-folds on the surface of trophozoites were filled with material present in the extracellular matrix (Fig. 9). The distinctive localization observed in *R. polygordiae* and *R. henneguyi* suggests that this deep but extracellular position is a homologous feature shared between them.

We found the putative sporozoites of *R. polygordiae* organized in large intracellular clusters within parasitophorous vacuoles of host intestinal epithelial cells (Fig. 20–27). Although speculative, we infer that once a cluster of infective sporozoites destroys an epithelial cell, the sporozoites develop into trophozoites, which now find themselves clustered in the extracellular matrix of the intestinal epithelium (Fig. 16).

Fig. **10–15.** Transmission electron micrographs (TEM) of the trophozoite cytoplasm in *Rhytidocystis polygordiae* n. sp. **10.** Low magnification TEM showing the major constituents of the cytoplasm: superficial vacuoles (v), paraglycogen granules (p), and lipid droplets (dark spots) (Bar = 2 μm). **11.** High magnification TEM showing Golgi bodies (Go), vacuoles (v), lipid droplets (l), and mitochondria (m) (Bar = 1 μm). **12.** High magnification TEM showing superficial vacuoles (v), mitochondria with tubular cristae (m), paraglycogen granules, lipid droplets (l), and a putative apicoplast (a) (Bar = 0.5 μm). **13.** High magnification TEM showing superficial vacuoles (v), mitochondria (m), paraglycogen granules, lipid droplets (l), the plasma membrane of a host intestinal epithelial cell (arrowhead), and the interstitial space between the trophozoite and the epithelial cells (asterisk) (Bar = 1 μm). **14.** TEM of a putative apicoplast showing four concentric membranes (Bar = 0.2 μm). **15.** High magnification TEM of the tripartite pellicle showing the outer plasma membrane and the two-layered inner membrane complex (Bar = 0.25 μm).

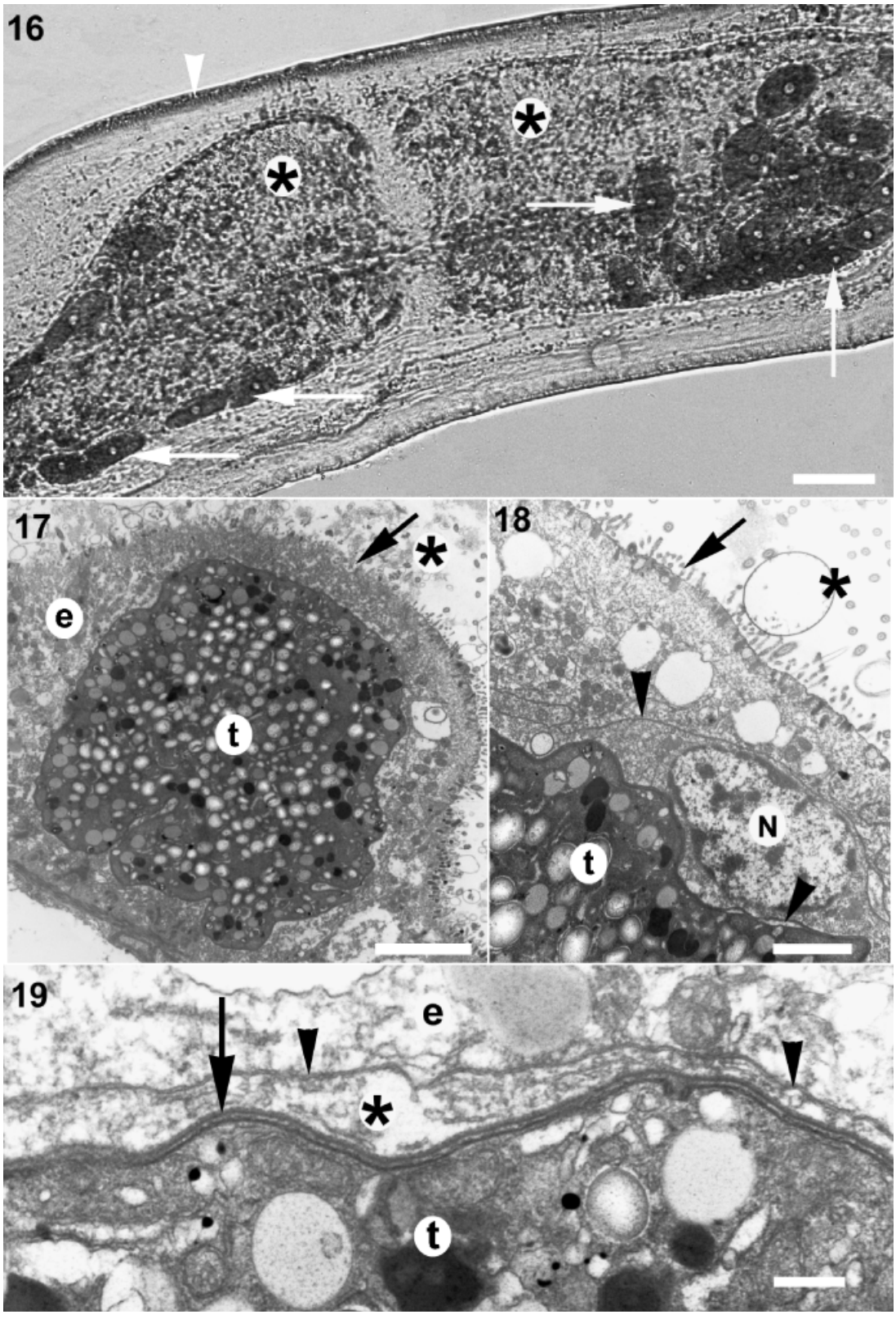
16
17
e
t
18
N
t
19
e
t

The overall structure of the sporozoites was typical of gregarines and eucoccidians (Desportes 1969; Porchet-Hennere 1972; Sheffield, Garnham, and Shiroishi 1971) (Fig. 20–27). For instance, the nucleus was positioned near the posterior end of the cell and contained condensed heterochromatin and a large nucleolus; the cytoplasm was filled with micronemes, dense granules, and a few club-shaped rhoptries (Fig. 23); the apical end contained a polar ring and conoid; one or two mitochondrial profiles had tubular cristae; and the endoplasmic reticulum was conspicuous. No unusual structures were observed, such as the crystalloid bodies of *R. sthenelais* or the flask-shaped structures (putative digestive vacuoles) of *Lankesteria culcis* (Porchet-Hennere 1972; Sheffield et al. 1971).

Although sexual reproduction has not been directly observed in *Rhytidocystis*, it has been described in *Gemmocystis* (de Beauchamp 1913; Levine 1979; Porchet-Hennere 1972; Upton and Peters 1986). Coelomic oocysts and sporocysts containing two sporozoites have been reported in a *R. opheliae*, *R. sthenelais*, and *R. henneguyi*. The latter also has trophozoites that are similar in morphology to those of *R. polygordiae* (de Beauchamp 1913; Levine 1979; Porchet-Hennere 1972) (Table 1). This suite of cyst-related characteristics is diagnostic for the Eucoccidia and is not known in gregarines or cryptosporidian parasites.

Molecular phylogeny. The phylogenetic relationships among 56 representative alveolates as inferred from SSU rDNA show the clade consisting of ciliates and the clade consisting of dinoflagellates+*Perkinsu*s supported with modest to strong bootstrap values and Bayesian posterior probabilities (Fig. 28). Although a clade consisting of colpodellids+apicomplexans was also consistently recovered, this group was weakly supported with bootstrap and Bayesian statistics. Within this group, colpodellids were paraphyletic and apicomplexans sensu stricto were weakly monophyletic. The weak statistical support recovered for the colpodellid+apicomplexan clade and the apicomplexan clade is consistent with previous studies of alveolate phylogeny using SSU rDNA (Cavalier-Smith and Chao 2004; Kuvardina et al. 2002; Leander et al. 2003a, b, c, 2006). Nonetheless, support for the apicomplexan clade is bolstered by ultrastructural characteristics (Cavalier-Smith and Chao 2004; Cox 1994; Leander and Keeling 2003; Levine 1988; Morrissette and Sibley 2002) and several phylogenetic studies of protein sequences (Fast et al. 2001, 2002; Harper, Waanders, and Keeling 2005; Leander and Keeling 2004; Leander et al. 2003a).

Most relationships near the origin of the Apicomplexa were unresolved. However, the following major clades can be inferred from current molecular and morphological evidence (Cavalier-Smith and Chao 2004; Leander et al. 2003b, 2006): (i) ''eucoccidia''+piroplasmids, (ii) cryptosporidian parasites, and (iii) septate eugregarines+marine aseptate eugregarines. As in previous studies, we did not recover a single clade that included only the eugregarine and neogregarine sequences. Instead, we recovered two gregarine clades, one consisting of the monocystid eugregarines (*Monocystis*) and the neogregarines (*Ophryocystis* and *Mattesia*), and another consisting of the septate eugregarines (*Gregarina* and *Leidyana*) and marine eugregarines (*Lecudina*, *Pterospora*, *Lithocystis*, and *Lankesteria*). All members of the latter clade share the property of having very divergent SSU rDNA sequences (Fig. 28).

Moreover, in a previous analysis of SSU rDNA, an undescribed apicomplexan clade consisting of environmental sequences CCI31, CCA38, and the marine parasite from *T. crocea* was identified as ''apicomplexan clade I'' (Leander et al. 2006). This clade, however, was not recovered when our new sequence from *R. polygordiae* was included in the analysis. Instead, *R. polygordiae* grouped strongly with the marine parasite from *T. crocea*, and the environmental sequences CCI31 and CCA38 grouped together with the archigregarine, *Selenidium terebellae* (albeit with weak support). We have termed the clade consisting of *R. polygordiae* and the marine parasite from *T. crocea* the ''rhytidocystids,'' implying that the latter is also a rhytidocystid. Only the sporozoites of the *Tridacna* parasite have been observed; they have a typical morphology and infect the hemocytes of their host (Nakayama, Nishijima and Maruyama, 1998). Whether the trophozoites and cysts of the *Tridacna* parasite are also similar to known rhytidocystids remains to be determined. Alternatively, the *Tridacna* parasite might be a closer relative to the gemmocystids of corals (Upton and Peters 1986), which appear to lack an obvious trophozoite stage.

The phylogenetic position of the rhytidocystid clade relative to other apicomplexans, especially eucoccidians and gregarines, is unclear. Nonetheless, the emerging phylogenetic pattern showing several lineages of archigregarines and archigregarine-like environmental sequences (e.g. *Selenidium terebellae* and environmental sequences CCA38, CC131, and BOLA 556) consistently branching near the origins of (i) the cryptosporidian clade, (ii) the rhytidocystid clade, and (iii) groups containing eugregarines+neogregarines, suggests that archigregarines form a paraphyletic stem group from which the aforementioned clades evolved independently of one another (Leander et al. 2006). Although this hypothesis is also consistent with morphological data (Grassé 1953; Kuvardina et al. 2002; Leander and Keeling 2003; Leander et al. 2003b, c, 2006; Schrével 1971a, b), a significant increase in the number and diversity of archigregarine sequences is needed to test its validity. This increased knowledge and taxon sampling will also help pinpoint the phylogenetic position of cryptosporidian parasites, which have shown a modest to strong affinity to certain gregarine lineages in both ribosomal and protein phylogenies (Carreno, Martin, and Barta 1999; Leander et al. 2003a, b, 2006). However, because the apicomplexan backbone is so poorly resolved in SSU rDNA trees, phylogenies inferred from different protein genes offer our best avenue for understanding the evolutionary histories of archigregarines, cryptosporidian parasites, and the newly characterized clade of rhytidocystids.

ACKNOWLEDGMENTS

We wish to thank three anonymous reviewers for feedback that significantly improved the manuscript. This work was supported by grants to B. S. L. from the Natural Sciences and Engineering Research Council of Canada (NSERC 283091-04) and from the

Fig. **16–19.** Light and electron micrographs of trophozoites showing *Rhytidocystis polygordiae* n. sp. in situ. **16.** Low magnification light micrograph of a host worm (arrowhead = body wall) showing the distribution of trophozoites (arrows) within the host (asterisks) (Bar = 65 μm). **17.** Low magnification transmission electron micrograph (TEM) of the intestinal wall (arrow) and lumen (asterisk) showing the position of the trophozoites (t) beneath the brush border of the epithelium (e) (Bar = 4 μm). **18.** Intermediate magnification TEM of the intestinal wall (arrow) and lumen (asterisk) showing the absence of an obvious parasitophorous vacuole and the position of the trophozoites (t) relative to the epithelial cells. The TEM shows the nucleus (N) and convoluted membranes between adjacent epithelial cells (arrowheads) (Bar = 2 μm). **19.** High magnification TEM showing putatively extracellular trophozoites (t) positioned within the interstitial spaces (asterisk) between epithelial cells (e). The interstitial space (asterisk) is defined by the plasma membrane of the trophozoite (arrow) and the plasma membrane of the adjacent epithelial cell (arrowheads) (Bar = 0.5 μm).

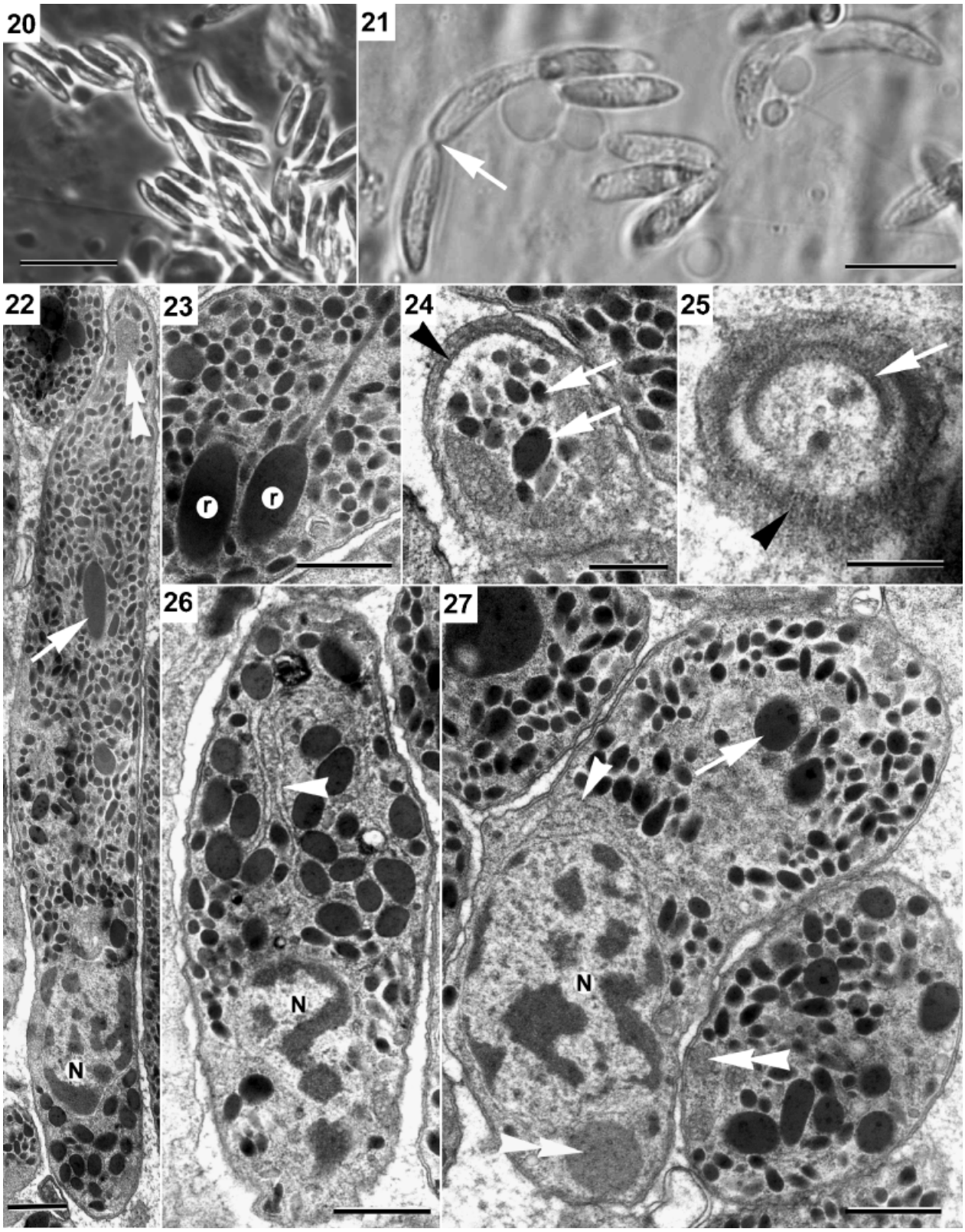
20
21
22
23
r
r
24
25
26
N
27
N
N

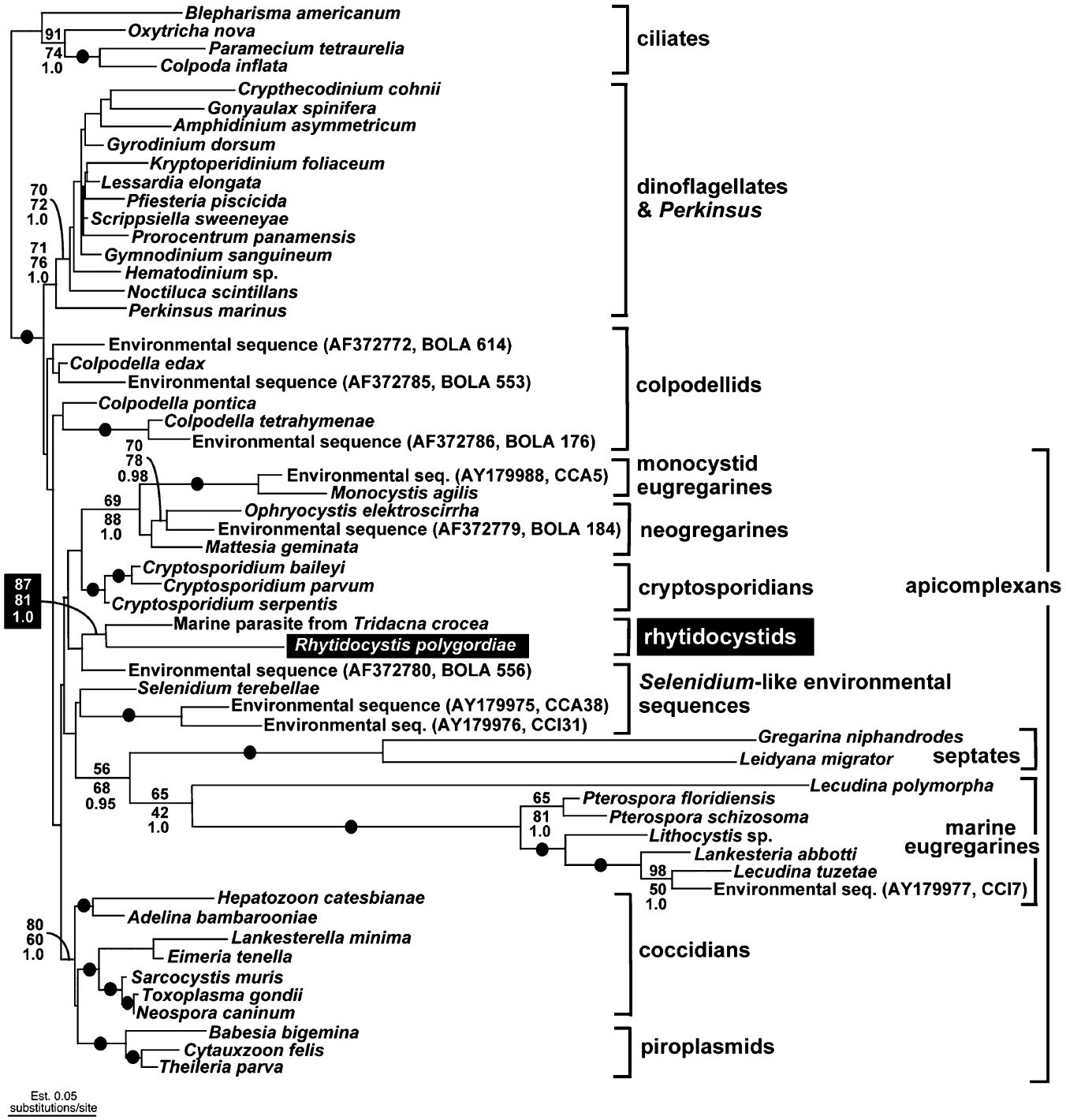

Fig. **28.** Gamma-corrected maximum likelihood tree ($-\ln L = 15172.715$, $\alpha = 0.38$, number of rate categories = 8) inferred using the general time reversible (GTR) model of substitution on an alignment of 56 small subunit (SSU) rDNA sequences and 1,159 sites. Numbers at the branches denote gamma-corrected bootstrap percentages using maximum likelihood—HKY (upper) and weighted neighbor-joining (middle). The lower number refers to Bayesian posterior probabilities—GTR. Black dots on branches denote bootstrap values and posterior probabilities above 85% in all analyses. The SSU rDNA sequence from *Rhytidocystis polygordiae* n. sp. is highlighted in a black box and is closely related to the largely uncharacterized parasite from giant clams (*Tridacna crocea*), together forming the rhytidocystid clade.

Fig. **20–27.** Light (LM) and transmission electron micrographs (TEM) of the spindle-shaped sporozoite stages in *Rhytidocystis polygordiae* n. sp. **20**, **21.** High magnification LMs of sporozoites released from disrupted oocysts in the coelom following host dissection. Occasionally, pairs of sporozoites were observed connected at the cell tips (arrow) (Bars = 15 and 10 μm, respectively). **22.** Longitudinal section of a sporozoite (apical end up) showing the posteriorly positioned nucleus (N) with condensed heterochromatin, a few large club-shaped rhoptries (arrow), an anteriorly positioned mitochondrion (double arrowhead), and cytoplasm full of micronemes and dense granules (smaller dark bodies) (Bar = 1 μm). **23.** High magnification TEM of two club-shaped rhoptries (r) (Bar = 1 μm). **24.** High magnification TEM of the apical complex showing micronemes in transverse section (arrows) and subpellicular microtubules (arrowhead) (Bar = 0.5 μm). **25.** Oblique section through the apical complex showing the conoid (arrow) and subpellicular structures (arrowhead) (Bar = 0.5 μm). **26, 27.** Oblique sections through sporozoites showing posteriorly positioned nuclei (N) with condensed heterochromatin, endoplasmic reticulum (arrowheads), rhoptry (arrow), and mitochondria (double arrows) (Bars = 1 μm).

Canadian Institute for Advanced Research (CIAR). P. A. R. was also supported by an IMCS graduate assistantship and graduate student research funds from Rutgers University Marine Field Station.

LITERATURE CITED

Beyer, T. V., Svezhova, N. V., Radchenko, A. I. & Sidorenko, N. V. 2002. Parasitophorous vacuole: morphofunctional diversity in different coccidian genera (a short insight into the problem). *Cell Biol. Int.*, **26**:861–871.

Bruno, W. J., Socci, N. D. & Halpern, A. L. 2000. Weighted neighbor joining: a likelihood-based approach to distance-based phylogeny reconstruction. *Mol. Biol. Evol.*, **17**:189–197.

Carreno, R. A., Martin, D. S. & Barta, J. R. 1999. *Cryptosporidium* is more closely related to the gregarines than to coccidia as shown by phylogenetic analysis of apicomplexan parasites inferred using small-subunit ribosomal RNA gene sequences. *Parasitol. Res.*, **85**: 899–904.

Cavalier-Smith, T. & Chao, E. E. 2004. Protalveolate phylogeny and systematics and the origins of Sporozoa and dinoflagellates (phylum Myzozoa nom. nov.). *Eur. J. Protistol.*, **40**:185–212.

Chen, X.-M., Keithly, J. S., Paya, C. V. & LaRusso, N. F. 2002. Cryptosporidiosis. *N. Engl. J. Med.*, **346**:1723–1731.

Cox, F. E. G. 1994. The evolutionary expansion of the sporozoa. *Int. J. Parasitol.*, **24**:1301–1316.

de Beauchamp, P. 1913. Recherches sur les *Rhytidocystis* parasities des Ophélies. *Arch. Protistenkd.*, **31**:138–168.

Desportes, I. 1969. Ultrastructure et developement des gregarines du genre *Stylocephalus*. *Ann. Sci. Nat. Zool.*, **11**:31–96.

Elliot, D. A. & Clark, D. P. 2000. *Cryptosporidium parvum* induces host-cell actin accumulation at the host-parasite interface. *Infect. Immun.*, **68**:2315–2322.

Fast, N. M., Kissinger, J. C., Roos, D. S. & Keeling, P. J. 2001. Nuclear-encoded, plastid-targeted genes suggest a single common origin for apicomplexan and dinoflagellate plastids. *Mol. Biol. Evol.*, **18**: 418–426.

Fast, N. M., Xue, L., Bingham, S. & Keeling, P. J. 2002. Re-examining alveolate evolution using multiple protein molecular phylogenies. *J. Eukaryot. Microbiol.*, **49**:30–37.

Felsenstein, J. 1993. PHYLIP (Phylogeny Inference Package). University of Washington, Seattle.

Giard, A. 1880. On the affinities of the genus *Polygordius* with the annelids of the family Opheliidae. *Ann. Mag. Nat. Hist.*, **6**:324–326.

Grassé, P.-P. 1953. Classe des grégarinomorphes (Gregarinomorpha n. nov.; Gregarinae Haeckel, 1866; gregarinidea Lankester, 1885; grégarines des auteurs). *In:* Grassé, P.-P. (ed.), Traité de Zoologie. Masson, Paris. p. 590–690.

Harper, J. T., Waanders, E. & Keeling, P. J. 2005. On the monophyly of chromalveolates using a six-protein phylogeny of eukaryotes. *Int. J. Syst. Evol. Microbiol.*, **55**:487–496.

Hennig, W. 1966. Phylogenetic Systematics. University of Illinois Press, London.

Huelsenbeck, J. P. & Ronquist, F. 2001. MrBayes: Bayesian inference of phylogenetic trees. *Bioinformatics*, **17**:754–755.

Kuvardina, O. N., Leander, B. S., Aleshin, V. V., Myl'nikov, A. P., Keeling, P. J. & Simdyanov, T. G. 2002. The phylogeny of colpodellids (Eukaryota, Alveolata) using small subunit rRNA genes suggests they are the free-living ancestors of apicomplexans. *J. Eukaryot. Microbiol.*, **49**:498–504.

Landers, S. C. 2002. The fine structure of the gamont of *Pterospora floridiensis* (Apicomplexa: Eugregarinida). *J. Eukaryot. Microbiol.*, **49**:220–226.

Lang-Unnasch, N., Reith, M. E., Munholland, J. & Barta, J. R. 1998. Plastids are widespread and ancient in parasites of the phylum Apicomplexa. *Int. J. Parasitol.*, **28**:1743–1754.

Leander, B. S. & Keeling, P. J. 2003. Morphostasis in alveolate evolution. *Trends Ecol. Evol.*, **18**:395–402.

Leander, B. S., Clopton, R. E. & Keeling, P. F. 2003a. Phylogeny of gregarines (Apicomplexa) as inferred from SSU rDNA and beta-tubulin. *Int. J. Syst. Evol. Microbiol.*, **53**:345–354.

Leander, R. S., Harper, J. T. & Keeling, P. J. 2003b. Molecular phylogeny and surface morphology of marine aseptate gregarines (Apicomplexa): *Selenidium* spp. and *Lecudina* spp. *J. Parasitol.*, **89**:1191–1205.

Leander, B. S., Kuvardina, O. N., Aleshin, V. V., Mylnikov, A. P. & Keeling, P. J. 2003c. Molecular phylogeny and surface morphology of *Colpodella edax* (Alveolata): insights into the phagotrophic ancestry of apicomplexans. *J. Eukaryot. Microbiol.*, **50**:334–340.

Leander, B. S. & Keeling, P. J. 2004. Early evolutionary history of dinoflagellates and apicomplexans (Alveolata) as inferred from hsp90 and actin phylogenies. *J. Phycol.*, **40**:341–350.

Leander, B. S., Lloyd, S. A. J., Marshall, W. & Landers, S. C. 2006. Phylogeny of marine gregarines (Apicomplexa)—*Pterospora*, *Lithocystis* and *Lankesteria*—and the origin(s) of coelomic parasitism. *Protist*, **157**:45–60.

Levine, N. D. 1979. Agamococcidiorida ord. n. and Rhytidocystidae fam. n. for the coccidian genus *Rhytidocystis* Henneguy, 1907. *J. Protozool.*, **26**:167–168.

Levine, N. D. 1988. The Protozoan Phylum Apicomplexa. CRC Press Inc., Boca Raton, FL.

Maddison, D. R. & Maddison, W. P. 2000. MacClade. Sinauer Associates Inc., Sunderland, MA.

McFadden, G. I. 2003. Plastids, mitochondria and hydrogenosomes. *In*: Marr, J. J., Nielsen, T. W. & Komuniecki, R. (ed.), Molecular Medical Parasitology. Academic Press, Boston. p. 277–294.

McFadden, G. I., Waller, R. F., Reith, M. E. & Lang-Unnasch, N. 1997. Plastids in apicomplexan parasites. *In:* Bhattacharya, D. (ed.), Plant Systematics and Evolution. Springer Verlag, Berlin. p. 261–287.

McIntosh, W. C. 1875. On a new example of the Opheliidae *Linotrypane apogon* from Shetland. *Proc. Royal Soc. Edinburgh*, **8**:386–390.

Morrissette, N. S. & Sibley, L. D. 2002. Cytoskeleton of apicomplexan parasites. *Microbiol. Mol. Biol. Rev.*, **66**:21–38.

Nakayama, K., Nishijima, M. & Maruyama, T. 1998. Parasitism by a protozoan in the hemolymph of the giant clam, *Tridacna crocea*. *J. Invertebr. Pathol.*, **71**:193–198.

Oborník, M., Jirku, M., Slapeta, J. R., Modry, D., Koudela, B. & Lukeš, J. 2002. Notes on coccidian phylogeny, based on the apicoplast small subunit ribosomal DNA. *Parasitol. Res.*, **88**:360–363.

Petry, F. 2004. Structural analysis of *Cryptosporidium parvum*. *Microsc. Microanal.*, **10**:586–601.

Porchet-Hennere, E. 1972. Observations en microscopie photonique et electronique sur la sporogenese de *Dehornia* (1) *sthenelais* (n. gen., sp. n.), sporozoaire parasite de l'annedlide polychaete *Sthenelais boa* (Aphroditides). *Protistologica*, **8**:245–255.

Posada, D. & Crandall, K. A. 1998. MODELTEST: testing the model of DNA substitution. *Bioinformatics*, **14**:817–818.

Ramey, P. A., Fiege, D. & Leander, B. S. 2006. A new species of *Polygordius* (Polychaeta: Polygordiidae): a dominant member of infaunal communities on the inner continental shelf and in bays and harbors of the northeastern United States. *J. Mar. Biol. Assoc. UK* (in press).

Rouse, G. W. & Pleijel, F. 2001. Polychaetes. Oxford University Press, London.

Schrével, J. 1968. L'ultrastructure de la région antérieure de la grégarine *Selenidium* et son intérêt pour l'étude de la nutrition chez les sporozoaires. *J. Microsc.*, **7**:391–410.

Schrével, J. 1971a. Observations biologiques et ultrastructurales sur les Selenidiidae et leurs conséquences sur la systématique des grégarinomorphes. *J. Protozool.*, **18**:448–470.

Schrével, J. 1971b. Contribution a l'étude des Selenidiidae parasites d'annélides polychètes. II Ultrastructure de quelques trophozoïtes. *Protistologica*, **7**:101–130.

Sheffield, H. G., Garnham, P. C. C. & Shiroishi, T. 1971. The fine structure of the sporozoite of *Lankesteria culcis*. *J. Protozool.*, **18**:98–105.

Strimmer, K. & Von Haeseler, A. 1996. Quartet puzzling: a quartet maximum likelihood method for reconstructing tree topologies. *Mol. Biol. Evol.*, **13**:964–969.

Swofford, D. L. 1999. Phylogenetic Analysis Using Parsimony (and Other Methods) PAUP* 4.0. Sinauer Associates Inc., Sunderland, MA.

Upton, S. J. & Peters, E. C. 1986. A new and unusual species of coccidium (Apicomplexa: Agamococcidiorida) from Jamaican scleractinian corals. *J. Invertebr. Pathol.*, **47**:184–193.

Vivier, E. 1968. L'organization ultrastructurale corticale de la gregarine *Lecudina pellucida*: ses repports avec l'alimentation et la locomotion. *J. Protozool.*, **15**:230–246.

Vivier, E. & Desportes, I. 1990. Phylum Apicomplexa. *In*: Margulis, L., Corliss, J. O., Melkonian, M. & Chapman, D. J. (ed.), The Handbook of Protoctista. Jones & Bartlett Publishers, Boston. p. 549–573.

Vivier, E. & Hennere, E. 1965. Ultrastructure des stades végétatifs de la coccidie *Coelotropha durchoni*. *Protistologica*, **1**:89–104.

Vivier, E. & Schrével, J. 1966. Les ultrastructures cytoplasmiques de *Selenidium hollandei*, n. sp. grégarine parasite de *Sabellaria alveolata* L. *J. Microsc.*, **5**:213–228.

Von Alt, C. J. & Grassle, J. F. 1992. LEO-15, an unmanned long-term environmental observatory. *Proc. Oceans '92*, **2**:849–854.

Waller, R. F. & McFadden, G. I. 2005. The apicoplast: a review of the derived plastid of apicomplexan parasites. *Curr. Issues Mol. Biol.*, **7**:57–80.

Warner, F. D. 1968. The fine structure of *Rhynchocystis pilosa* (Sporozoa, Eugregarinida). *J. Protozool.*, **15**:59–73.

Wray, C. G., Langer, M. R., DeSalle, R., Lee, J. J. & Lipps, J. H. 1995. Origin of the foraminifera. *Proc. Natl. Acad. Sci. USA*, **92**:141–145.

Zhu, G., Marchewka, M. J. & Keithly, J. S. 2000. *Cryptosporidium parvum* appears to lack a plastid genome. *Microbiology*, **146**:315–321.

Received: 11/04/05, 01/06/06, 02/03/06, 04/04/06; accepted: 04/04/06